Electron Bernstein Wave Assisted Plasma Current Start-up in MAST

V.F. Shevchenko, M.R. O'Brien, D. Taylor and MAST team
*EURATOM/UKAEA Fusion Association, Culham Science Centre, Abingdon, OX14 3DB, UK**

A.N. Saveliev
Ioffe Institute, Politekhnicheskaya 26, 194021 St.Petersburg, Russia

(Dated: September 8, 2009)

Electron Bernstein wave (EBW) assisted plasma current start-up has been demonstrated for the first time in a tokamak. It was shown that plasma currents up to 17 kA can be generated non-inductively by 100 kW of RF power injected. With optimized vertical field ramps, plasma currents up to 33 kA have been achieved without the use of solenoid flux. It is shown that the plasma formation and current generation are governed predominantly by EBW current drive. Experimental results are consistent with ray-tracing and quasilinear Fokker-Planck modeling.

PACS numbers: 52.35.Hr, 52.50.Fa, 52.50.Sw

Non-inductive plasma current start-up is a critical issue in spherical tokamak (ST) research because of lack of space for a shielded central solenoid. Various techniques have been proposed and developed in order to avoid a central solenoid in future ST devices [1–5]. In this Letter, we report on the electron Bernstein wave (EBW) start-up technique based on a 28 GHz gyrotron capable of delivering 100 kW power for up to 90 ms [6]. Experiments were carried out on the Mega Amp Spherical Tokamak (MAST) at Culham Science Centre, UK. The EBW start-up method deployed here relies on the production of low-density plasma by RF pre-ionization around the fundamental electron cyclotron resonance (ECR). Then a double mode conversion (MC) is considered for EBW excitation. The scheme consists of MC of the ordinary (O) mode, incident from the low field side of the tokamak, into the extraordinary (X) mode with the help of a grooved mirror-polarizer incorporated in a graphite tile on the central rod (CR). The launched gaussian beam is tilted to the midplane at 10^o and hits the CR at the midplane as illustrated in Fig. 1. The O-mode beam has an effective (electric field e-fold length) radius of about 80 mm which is well within the grooved area of 250×250 mm^2 on the CR. The X mode reflected from the polarizer propagates back to the plasma passes through ECR and experiences a subsequent X to EBW MC near the upper hybrid resonance (UHR). Finally the excited EBW mode is totally absorbed before it reaches the ECR, due to the Doppler shifted resonance. The absorption of EBW remains high even in cold rarefied plasmas [7]. Furthermore, EBW can generate significant plasma current (if absorption is above or below the midplane) [8] during the start-up phase giving the prospect of a fully non-inductive plasma start-up.

An important part of any start-up scenario is a transition from the open field line configuration to the closed flux surfaces (CFS) formation. A spontaneous formation

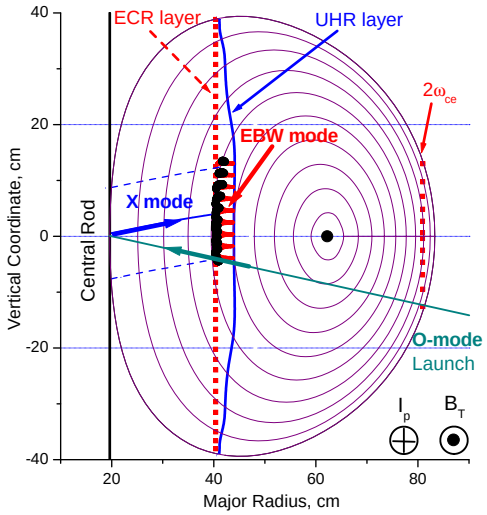

FIG. 1: Schematic of the EBW assisted plasma current start-up. Poloidal projection of EBW ray-tracing based on the plasma equilibrium reconstructed from experimental data. Black areas represent EBW damping.

of CFS has been observed in a number of RF assisted start-up experiments [1, 3, 5]. Different mechanisms driving CFS formation have been proposed. It will be shown that in EBW assisted start-up experiments the CFS formation is mainly governed by EBW current drive (CD). First let us consider start-up in a constant vertical field. The toroidal field value was set by the CR current of 2.05 MA giving an ECR radial position of 41 cm. The vertical field was induced by a pair of coils 3 m in diameter located 1.1 m above and below the midplane. These coils were energized with -10 kA·turn current producing a vertical field B_V = -2.3 mT at the ECR in the midplane. The vessel was pre-filled with deuterium using a pulsed valve 10 ms prior to RF injection. In this set-up the injected RF power causes breakdown followed by a quick accumulation of the plasma around the CR near the midplane. In the case of high pre-fill the plasma reached the

*Electronic address: vladimir.shevchenko@ukaea.org.uk

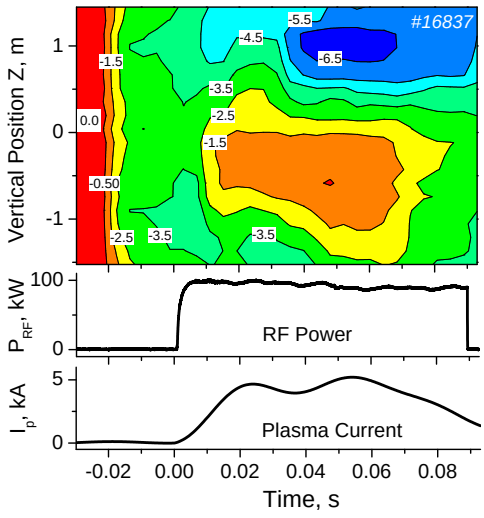

FIG. 2: Contour map of the vertical component of the magnetic field measured on the central rod in mT.

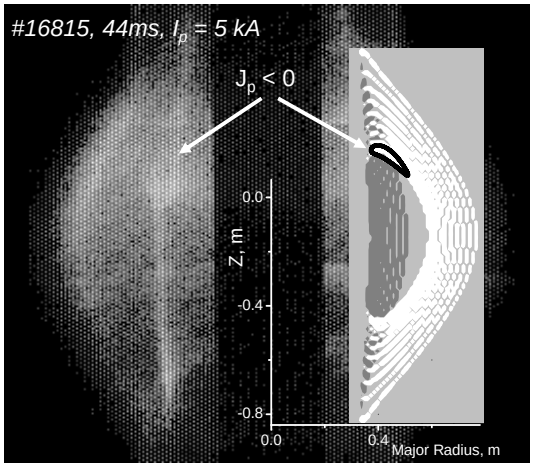

FIG. 3: CCD image of the EBW start-up shot and drift orbit simulations. Note the electron has to execute multiple toroidal turns while completing a single banana orbit. It is carrying co-current on the outboard side of the orbit and counter-current on the inboard side.

O-mode cut-off density ($n_{e0} = 10^{19}\ m^{-3}$ for 28 GHz) causing strong reflection of the RF power back to the gyrotron. Therefore we consider only low density plasmas in which the O-mode cut-off was not reached. The plasma density increase near the midplane was accompanied by plasma current generation. The plasma current increased for the first 20-30 ms and then gradually decayed to zero. Experiments were conducted with pulsed and continuous gas puffs over a range of plasma densities with B_V ramped up and down in time. The maximum current achieved was about 10 kA and it could not be sustained for longer than 50 ms. The vertical component of the magnetic field at the CR showed interesting behavior in this set of experiments. The field was measured with an array of 40 magnetic probes incorporated into the graphite shielding on the CR. A contour map of B_V against time and vertical coordinate is shown in Fig. 2. As seen from this figure the measured field is zero until the B_V coils energized at -20 ms. The field produced by the B_V coils alone is negative and its value does not exceed 4 mT at any vertical position on the CR. The pressure driven current appears during the density increase and it causes a decrease of B_V near the midplane. For the first 5 ms after appearance of the current, the field induced by this current is quite symmetrical about the midplane. Then the plasma current starts to move down. At the same time a zone with $B_V \leq$ -4 mT, more negative than produced by the B_V coils, appears above Z=0.5 m. It can only be produced by the current flowing in a counter direction. After that moment two zones carrying opposite currents move further apart causing gradual termination of the plasma well before the end of the RF pulse. Fast video images of the plasma show the appearance of a bright ring at the moment when the negative current occurs (see Fig. 3). It is then followed by a gradual increase of plasma elongation until termination. Variations in gas puffing and B_V ramps affected only the timing of the events while the sequence remained the same. CFS formation was not observed in these preliminary experiments.

In order to explain this phenomenon let us analyse single particle orbits during the start-up phase. The importance of such analysis has been noted in [5]. The numerical formalism used in our simulations is very similar to the method described in [9]. For the densities typical during the negative current appearance the UHR layer is located near R = 0.45 m. The RF beam centre crosses this layer and the ECR at about 5 cm above the midplane as seen in Fig. 1. These cross-sections define the origin of the test particles in our modeling. As a result of resonance interaction electrons acquire an energy of about 5 keV [10] predominantly due to an increase of the velocity $v_\perp$ perpendicular to the magnetic field. The electron temperature measured with Thomson scattering (TS) along magnetic field does not exceed 50 eV during an initial phase of the discharge. Thus, electrons with an energy of 5 keV and pitch angles corresponding to $-0.1 < v_\parallel/v_\perp < 0.1$ were considered in simulations. It was found that banana orbits are dominant in MAST for both co- and counter- launched electrons in the above range of pitch angles and energy. Assuming the number of electrons generated at a particular height is proportional to the absorbed RF power, the resultant current was integrated over the range of orbits. The grey-scale contour map in Fig. 3 represents a poloidal cross-section of the current density generated by banana trapped particles. The areas darker than the background colour correspond to counter-current while the whiter areas correspond to co-current. The total current integrated over the cross-section shown in Fig. 3 is about 3 kA. It is always positive for MAST parameters. There is also a positive current carried by selectively confined passing electrons accumu-

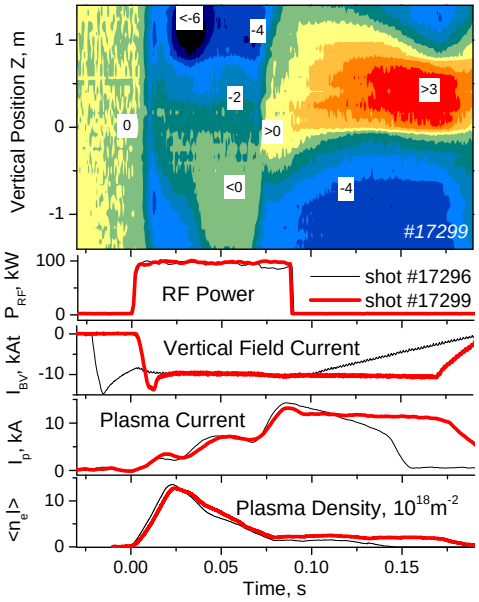

FIG. 4: Same as in Fig. 2. Negative current suppression by radial field applied during the shot. Black waveforms illustrate the effect of B_V timing on plasma current generation.

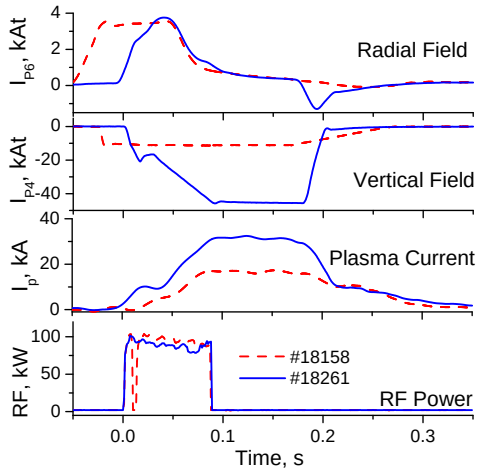

FIG. 5: Waveforms during EBW assisted non-solenoid plasma current start-up with constant B_V (red dashes) and with optimized B_V ramp-up.

lated from the thermal bulk [5, 9]. These currents contribute to the poloidal field. It was found that starting from plasma currents of 2 kA, carried predominantly by trapped electrons, the curvature of the field does change its sign. The field with modified curvature allows the existence of passing orbits carrying negative current [11]. Fig. 3 illustrates such an orbit localized on the upper half-plane. In general these orbits destroy up-down symmetry of the plasma if there is an asymmetry in the fast particle source. It was concluded the above mechanism is responsible for the negative current sustainment. The similarity between simulated orbits and the plasma image taken during the decay phase supports this conclusion.

The wave vector k_{EBW} of mode converted EBW is essentially perpendicular to the UHR layer due to a very large component of refractive index perpendicular to the magnetic field ($N_\perp \sim 100$) and small parallel $N_\parallel << 1$ component. The sign of $N_\parallel$ is determined by the projection of k_{EBW} on the local poloidal magnetic field. $N_\parallel$ does not change sign along the ray trajectory except for propagation near the midplane [12]. As the wave approaches ECR $N_\parallel$ gradually increases and the condition $\mid N_\parallel \mid \geq 1$ is often reached near ECR. The sign of $N_\parallel$ determines whether the wave interacts with electrons moving along or opposite to the magnetic field. In the open field line configuration the curvature of the UHR layer in the MC zone is larger than the local curvature of B_V lines in the range of plasma densities during start-up. This results in $N_\parallel < 0$ above the midplane and $N_\parallel > 0$ below. Such a combination of $N_\parallel$ signs supports negative plasma current (by direct acceleration of electrons carrying negative current) above the midplane and positive below as was observed in experiments. The sign of $N_\parallel$ can be controlled by changing the local curvature of B_V, for example, by shifting the B_V minimum upward providing favorable $N_\parallel$ in the MC zone. This was achieved with the help of radial magnetic field coils. Fig. 4 illustrates negative current suppression followed by CFS formation. Here the radial field was applied throughout the shot. It produced an up-shift of the plasma of about 20 cm providing predominant $N_\parallel > 0$ in the MC zone. The negative current appeared only briefly with a maximum at about 25 ms then it was suppressed by expanding positive current finally leading to CFS formation near the midplane. The appearance of CFS is indicated by the B_V reversal at CR at 75 ms followed by further increase of the plasma current. After CFS formation $N_\parallel$ changes its sign in the MC layer due to the B_V reversal. In order to switch EBW CD to co-direction the plasma must be down-shifted back to the midplane. After down-shift timing optimization plasma currents up to 17 kA have been achieved with constant B_V and RF power alone as illustrated in Fig. 5. Fig. 5 shows also a shot with optimized B_V ramps when plasma current of 33 kA has been achieved. Here the first B_V ramp is applied to assist the initial current generation and the second ramp is necessary to keep the plasma in equilibrium while the plasma current is rising.

Fig. 6 shows a CCD image of the plasma with superimposed magnetic equilibrium reconstruction. Fig. 7 represents electron density and temperature profiles measured by TS after additional gas puffing at the end of RF injection. It can be seen from these figures that the generated plasma consists of a hot toroidal core with the maximum $T_e \sim 0.7$ keV and density $n_e \sim 1.5 \cdot 10^{18} m^{-3}$. A predominant fraction of the current is flowing within the core as indicated from the magnetic reconstruction. Outside the toroidal core there is a relatively cold plasma which consists of trapped particles also carrying a small fraction $< 10\%$ of the plasma current which was not accounted in

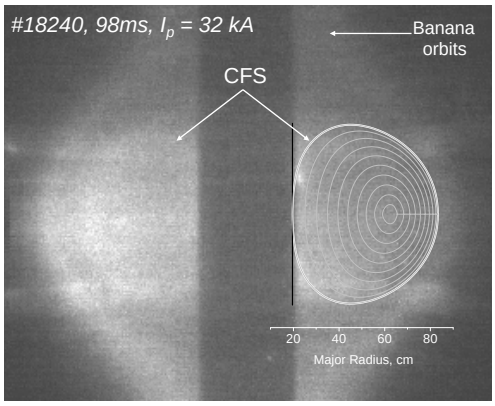

FIG. 6: CCD image of the plasma with formed CFS and magnetic equilibrium reconstruction on the right.

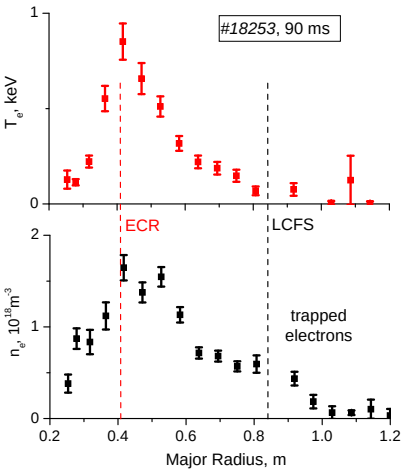

FIG. 7: Electron temperature and density profiles measured with TS. Optimized B_V ramp-up, $I_p = 32kA$.

reconstruction. From Fig. 5 one can see that the plasma current remains slowly decaying for a long time after the end of the RF pulse. Experimentally observed time scales are in the range of 0.4 - 0.5 s. The decay time can be significantly shortened by additional gas puffing. This fact suggests that the plasma current is carried predominantly by supra thermal electrons. Their energy estimated from the measured slowing down time must be in the range of 70-100 keV. This suggestion is supported by the ray-tracing and Fokker-Planck modeling [13] conducted for start-up plasmas with formed CFS. Plasma currents from 30 to 50 kA are predicted by modeling for the range of achieved plasma parameters. Fig. 8 shows the electron distribution function disturbed by the resonance interaction with EBW. Interestingly, the most noticeable generation of fast electrons is observed for waves with $N_\parallel = 1$. That is the so-called "auto resonance regime" [14] which provides a mechanism for effective electron acceleration to supra thermal energies. In the present geometry (see Fig. 1) $N_\parallel$ is close to 0 for the EBW rays propagating near the midplane. The rays originated at the top of the MC

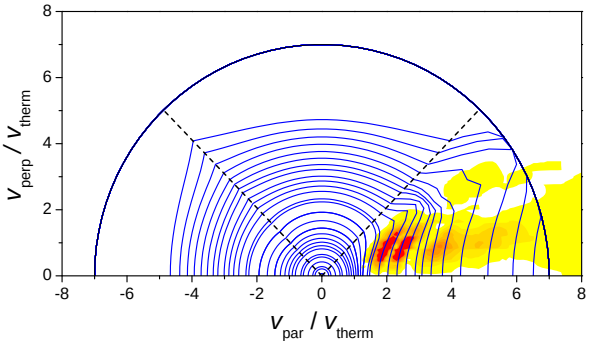

FIG. 8: Fokker-Planck modeling results for equilibrium as in Fig. 1 and profiles as in Fig. 7. Contours of the electron distribution function and color map of the quasilinear diffusion operator calculated for EBWs.

zone in cold plasmas acquire $N_\parallel > 1$ at the ECR. Thus the waves with $N_\parallel = 1$ satisfying auto resonance conditions are always present during initial phase of plasma formation. Auto resonance might be responsible for the production of fast electrons in EBW assisted plasma current start-up.

This work has been funded jointly by the United Kingdom Engineering and Physical Sciences Research Council and by the European Communities under the contract of association between EURATOM and UKAEA. The views and opinions expressed in this paper do not necessarily reflect those of the European Commission.

[1] C.B. Forest, *et al.*, Phys. Rev. Lett. **68**, 3559 (1992).
[2] R. Raman, *et al.*, Phys. Rev. Lett. **90**, 075005 (2003).
[3] A. Ejiri, *et al.*, Nucl. Fusion **46**, 709 (2006).
[4] M. Gryaznevich, *et al.*, Nucl. Fusion **46**, S573 (2006).
[5] T. Yoshinaga, *et al.*, Phys. Rev. Lett. **96**, 125005 (2006).
[6] V. Shevchenko, *et al.*, Fusion Sci. Techn. **52**, 202 (2007).
[7] V. Petrillo, *et al.*, Plasma Phys. Contr. Fusion **29**, 877 (1987).
[8] V. Shevchenko, *et al.*, Phys. Rev. Lett. **89**, 265005 (2002).
[9] A. Ejiri and Y. Takase, Nucl. Fusion **47**, 403 (2007).
[10] M. Peng, *et al.*, Nucl. Fusion **18**, 1489 (1978).
[11] J. Egedal, Nucl. Fusion **40**, 1597 (2000).
[12] A. Piliya, *et al.*, Plasma Phys. Contr. Fusion **47**, 379 (2005).
[13] A.N. Saveliev, in Proceedings of the Joint Varenna-Lauzanne Int. Workshop on Theory of Fusion Plasma, Varenna, 2006, CP871, 215.
[14] A. Zvonkov, *et al.*, Plasma Phys. Reports **24**, 389 (1998).